

## Supporting information for

# Parallel Comparative Studies on Composition-dependent Peroxidase-like Catalytic Activity of Ultrasmall Ferrite Nanoparticles

Chunchao Xia<sup>1</sup>, Huan Zhang<sup>2, 3, 4\*</sup>, Mengmeng Xie<sup>2</sup>, Jiaying Che<sup>2</sup>, Quanqing Feng<sup>2</sup>,  
Yihan Zhang<sup>2</sup>, Guohang Ma<sup>2</sup>, Minrui Liu<sup>4</sup>, Sixian Hu<sup>1</sup>, Yuan He<sup>2</sup>, Xiaoli Liu<sup>5</sup>, Zhenlin  
Li<sup>1\*</sup>, Haiming Fan<sup>2\*</sup>

1 Department of Radiology, West China Hospital, Sichuan University, China

2 Center for Nanomedicine and Engineering, Key Laboratory of Synthetic and Natural  
Functional Molecule of the Ministry of Education, College of Chemistry and Materials  
Science, Northwest University, Xi'an 710127, China.

3 Department of Radiology, Zhuhai People's Hospital (The Affiliated Hospital of  
Beijing Institute of Technology, Zhuhai Clinical Medical College of Jinan University),  
Zhuhai 519000, China.

4 Key Laboratory of Birth Defects and Related Diseases of Women and Children,  
Ministry of Education, West China Second University Hospital, Sichuan University,  
Chengdu, 614001, China.

5 National Local Joint Engineering Research Center for Precision Surgery &  
Regenerative Medicine, First Affiliated Hospital of Xi'an Jiaotong University, Xi'an  
710061, China.

\*Address correspondence to Huan Zhang, zhanghuan62954@163.com; Zhenlin Li,  
HX\_lizhenlin@126.com; Haiming Fan, fanhm@nwu.edu.cn.

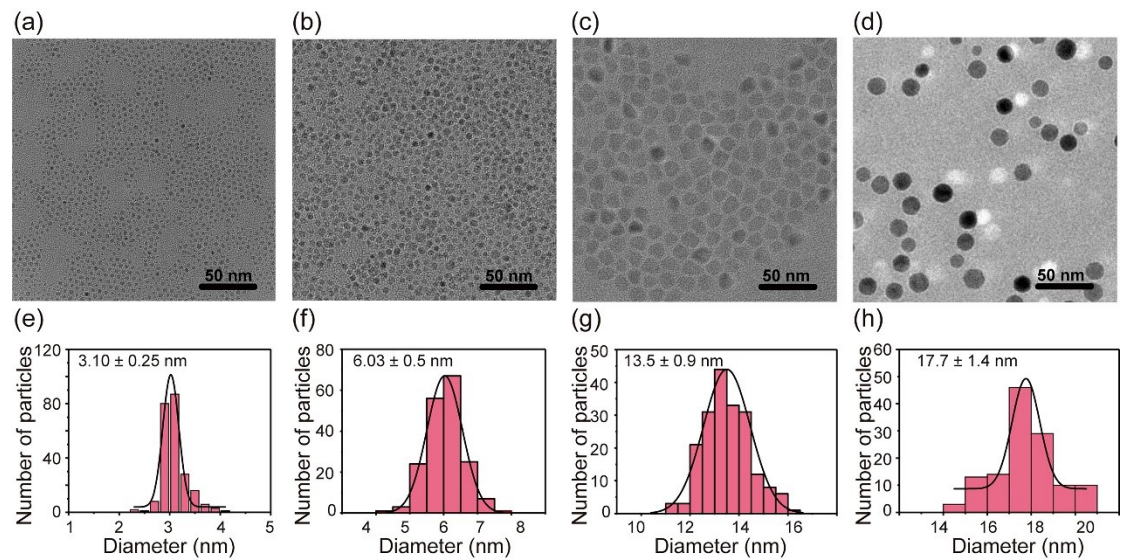


**Figure S1.** TEM images and the particle size distribution histograms of (a) (e) 3 nm, (b) (f) 6 nm, (c) (g) 14 nm and (d) (h) 18 nm sized  $\text{CoFe}_2\text{O}_4$  nanoparticles.

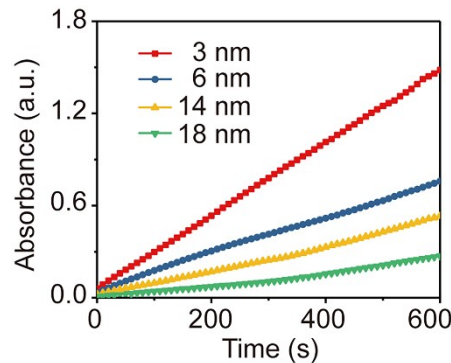


**Figure S2.** Time-dependent UV-vis absorbance changes at 652 nm of the TMB- $\text{H}_2\text{O}_2$  reaction system catalyzed by 3 nm, 6 nm, 14 nm, and 18 nm sized ferrite nanoparticles.

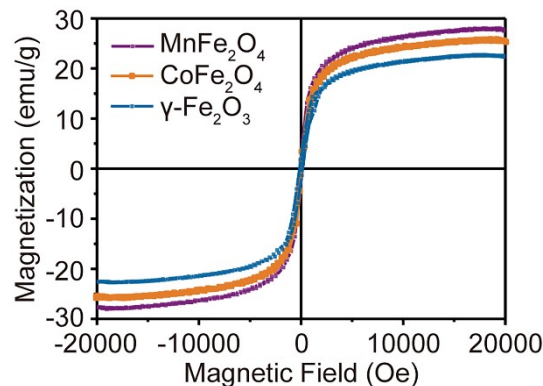


**Figure S3.** Hysteresis loop of the  $\text{CoFe}_2\text{O}_4$ ,  $\text{MnFe}_2\text{O}_4$ , and  $\gamma\text{-Fe}_2\text{O}_3$  nanoparticles at room temperature.

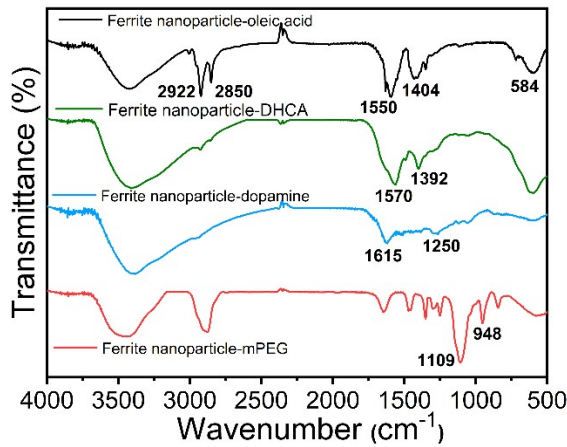


**Figure S4.** Fourier transform infrared spectroscopy (FTIR) for the ferrite nanoparticles before and after surface modification using dopamine, DHCA, and PO-mPEG ligands.

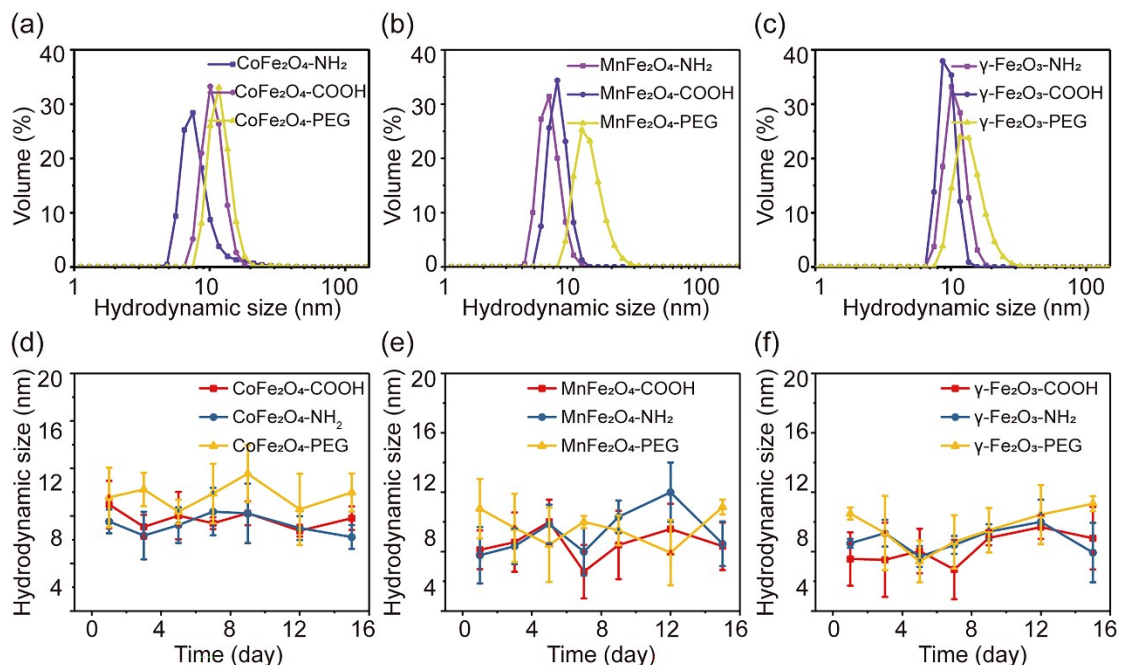


**Figure S5.** Hydrodynamic diameters of the dopamine, DHCA and PO-mPEG modified (a)  $\text{CoFe}_2\text{O}_4$ , (b)  $\text{MnFe}_2\text{O}_4$  and (c)  $\gamma\text{-Fe}_2\text{O}_3$  nanoparticles. Hydrodynamic size variation of the dopamine, DHCA and PO-mPEG modified (d)  $\text{CoFe}_2\text{O}_4$ , (e)  $\text{MnFe}_2\text{O}_4$  and (f)  $\gamma\text{-Fe}_2\text{O}_3$  nanoparticles as a function of time upon incubation in water.

**Table S1** Zeta potential of ultrasmall  $\text{CoFe}_2\text{O}_4$ ,  $\text{MnFe}_2\text{O}_4$  and  $\gamma\text{-Fe}_2\text{O}_3$  nanoparticles with the surface modification of dopamine, DHCA and PO-mPEG.

	$\text{CoFe}_2\text{O}_4$	$\text{MnFe}_2\text{O}_4$	$\gamma\text{-Fe}_2\text{O}_3$
<b>Dopamine</b>	30.6	30.4	29.0
<b>DHCA</b>	-28.0	-33.7	-34.7
<b>PO-mPEG</b>	5.4	11.4	6.6

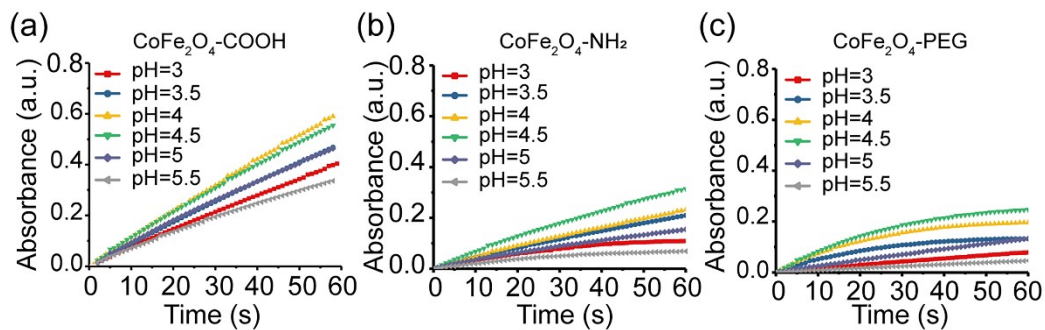


**Figure S6.** Time-dependent UV-vis absorbance changes at 652 nm of the TMB- $\text{H}_2\text{O}_2$  reaction system catalyzed by (a) DHCA (b) dopamine and (c) PO-mPEG modified  $\text{CoFe}_2\text{O}_4$  nanoparticles at the pH range from 3 to 5.5.

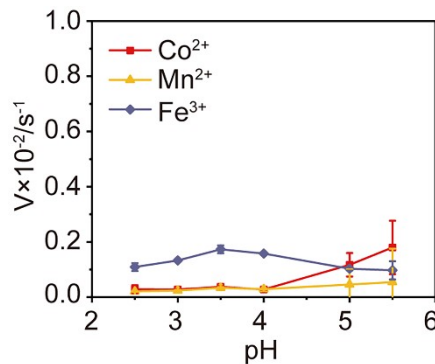


**Figure S7.** Peroxidase activity of dissociative  $\text{Co}^{2+}$ ,  $\text{Mn}^{2+}$  and  $\text{Fe}^{3+}$  were measured under standard conditions at a range of pH values from 2.5 to 5.5.